Span-60-Based Organogels as Probable Matrices for Transdermal/Topical Delivery Systems

B. Behera, V. Patil, S. S. Sagiri, K. Pal, S. S. Ray

Department of Biotechnology and Medical Engineering, National Institute of Technology, Rourkela, Orissa 769008, India

Received 29 May 2011; accepted 20 September 2011
DOI 10.1002/app.35674
Published online 28 December 2011 in Wiley Online Library (wileyonlinelibrary.com).

ABSTRACT: The current study describes the preparation and characterization of thermoreversible span-60 and sunflower oil (SO)-based organogels as a matrix for drug delivery. Effect of gelator concentration on the properties of the organogels was studied by physical property evaluation, stability, light microscopy, FTIR spectroscopy, XRD, thermal analysis, pH, and hemocompatibility studies. The drug release kinetics and antimicrobial efficacy of the salicylic acid loaded organogels were studied. The rate of gelation of the gels was found to be quicker in organogels with higher gelator proportions. The gels were inherently stable when stored below 25°C. The micrographs indicated the presence of needle-shaped crystals which formed aggregates resulting in the formation of three-dimensional networked structures. FTIR indicated intermolecular hydrogen bonding amongst SO and span-60 molecules responsible for the gelation. There was an increase in the crystallinity and the melting point of the organogels as the proportion of the organogelator was increased. The pH of the organogels indicated nonirritant nature of the gels, which were also found to be hemocompatible. The release of SA from organogels followed Higuchian kinetics and showed prolonged antimicrobial activity. The preliminary results indicated that the organogels may be tried as a matrix for controlled drug delivery. © 2011 Wiley Periodicals, Inc. J Appl Polym Sci 125: 852–863, 2012

Key words: Span-60; sunflower oil; salicylic acid; hemocompatible; transdermal/dermal delivery

INTRODUCTION

Organogels may be defined as a nonglassy thermoreversible semi-solid system containing an oil continuous phase (e.g. hexane, isopropyl myristate, SO, and corn oil), immobilized within a three-dimensional networked structure.[1–4] Gelators commonly used for the preparation of organogels include lecithin, sterols, cholesteryl anthraquinone derivatives, and fatty acid esters, such as sorbitan esters. [4–8] The use of organogels-based products as a matrix for delivery of bioactive agents is increasing exponentially. [9–13] This may be attributed to the easy method of preparation and inherent long-term stability of these products. [14] Depending on the mechanism of the formation of the three-dimensional skeleton, which help in immobilizing the apolar phase, the organogels are further categorized as fluid-filled structure and solid-fiber-based organogels. [15,16] Till recent past, most of the organogel-based products were developed using nonbiocompatible components. But with the advancement in the pharmaceutical, food, nutraceutical, and cosmetics industries, various organogel-based products are being developed using biocompatible components which are used for human applications. [9,17] Organogels containing span-60 have been tried successfully to deliver many bioactive agents (e.g., bovine serum albumin, hemagglutinin, aceclofenac, and contraceptive steroids) in a controlled way. [18–20]

Edible oil (e.g., SO and corn oil) are considered as multicomponent organic solvent containing high amount of unsaturated triacylglycerols (TAGs).[21] TAGs are often associated with low cardiovascular risk. SO, obtained from dried kernels of *Helianthus annuus*, is commonly available as used edible oil at low prices, and hence was used as the apolar phase in the study. It contains many antioxidant and anticarcinogenic chemical moieties apart from vitamin-E. [22–25]

Escherichia coli (*E. coli*), a gram negative bacteria, is responsible for many clinical infections (e.g., cholecystitis, bacteremia, urinary tract infections, travelers diarrhea, neonatal meningitis, and pneumonia).[26] *Bacillus subtilis* (*B. subtilis*), a gram positive bacteria, is often associated with dysentery.[27] In this study, the developed span-60- and SO-based gels were

Correspondence to: K. Pal (pal.kunal@yahoo.com).
Contract grant sponsor: Department of Biotechnology, Government of India; contract grant number: BT/PR14282/PID/06/598/2010.
Contract grant sponsor: National Institute of Technology-Rourkela, India.

evaluated for their ability to be an antimicrobial drug carrier.

MATERIALS AND METHODS

Materials

Span-60 (sorbitan monostearate) was purchased from Loba chemie, Mumbai, India. Salicylic acid (SA) was purchased from Sara fine chemicals, India. Edible refined SO was purchased from the local market. Dialysis tubing (MW cutoff: 60 kDa) was purchased from Himedia, Mumbai, India. All experimental studies were carried out using double distilled water.

Methods

Preparation of organogels

Accurately weighed span-60 flakes was dispersed in specified amount of SO. The proportion of span-60 was varied from 1–25 % (w/w). The mixture was heated at 60°C and stirred at 500 rpm in a magnetic stirrer-cum-hot plate, until span-60 completely dissolved to form a clear homogenous solution. The solution, so obtained, was allowed to cool to room-temperature (RT). If the cooled solution failed to flow under gravity when the vials were inverted, the solutions were regarded as gels. [28,29] Critical gelation concentration (CGC), the lowest concentration of gelator which induced gelation of SO, was determined.[30] For drug loaded organogels, SA (a model drug) was dissolved in SO such that the final product had 1% (w/w) of SA. The rest of the procedure was same. All the samples were kept at RT for further analysis.

Organoleptic evaluation

Freshly prepared organogels samples were observed for their color, odor, taste, appearance, and texture.

Accelerated aging test

Thermocycling is one of the accepted methods to simulate the aging by inducing stress in the pharmaceutical formulations.[31] The physical property like the appearance and texture was evaluated using this method. Freshly prepared organogel samples were subjected to 16 freezing–thawing cycles, by keeping them alternatively at temperature −20 and 60°C, respectively, for 15 min each. The study was continued up to 8 h. Samples were analyzed visually after each 15 min for any destabilization. A sample may be regarded as stable, if it withstands at least 5 cycles of thermo-cycling.

Stability studies on time scale

The accelerated stability test was performed as per the ICH guidelines.[32] Organogel samples were stored at RT, 5 and 37°C and were observed at regular intervals for any signs of destabilization for a period of 12 months.

Visual determination of gel–sol transition time

Gel (nonflow)–sol (flow) transition was determined using the inverting tube method. Organogels were heated in a temperature-controlled water-bath as the temperature was varied from 30 to 60°C at an increment of 2°C. The samples were equilibrated for 5 min at the previous temperature for 5 min before the temperature increment was made. The gel–sol transition was analyzed by inverting the vial after each incubation period.[28,29] The temperature at which samples started to flow was recorded as gel–sol transition temperature (T_g). All the experiments were carried out in duplicate.

Microscopic analysis

A compound optical microscope (Olympus CH20 i) was used for analyzing the microstructure of the organogels. Attempts were made to understand the organogel microstructure by varying the proportions of span-60 in gels.

Fourier transform infra red spectroscopy

Infrared spectroscopy of the samples was carried out by using ATR-FTIR instrument (Alpha-E by Brucker). The raw materials, representative blank organogel and representative SA-loaded organogel were scanned in the range of 3500 cm^{-1} to 500 cm^{-1} to understand the interactions amongst the components of the organogel.[33,34]

XRD analysis

The samples were subjected to XRD analysis using Philips, XRD-PW 1700, Rockville. Cu-Kα was used as the source, which was operating at 35 KV and 30 mA. Samples were scanned in the range of 10–50° 2θ at a rate of 2° 2θ per min.

Opacity measurement

The organogels were heated at 70°C and were subsequently cooled down at RT. The turbidity of the solution was measured using colorimeter (EI-D10 Digital Photo colorimeter). The change in turbidity of the solution was monitored at 400 nm using digital photo-colorimeter (EI Instruments India. model 312) either as a function of time or temperature.

Thermal analysis

Thermal properties of organogels were studied using simultaneous thermogravimetric analysis -differential thermal analysis (TGA-DTA; TA 60WS thermal analyzer, Shimadzu, Japan) and differential scanning calorimetry (DSC; STA 449C Jupiter, Netzsch, Germany). For simultaneous TGA-DTA analysis, samples were heated from 27°C up to 250°C, at a rate of 6°C/min. For DSC analysis, the samples were subjected to heating in the temperature range of 20–80°C, at a rate of 279.15 k/min.

pH measurement

The pH of organogel samples were detected by using digital ATC pH meter (EI instruments, model no-132E). The pH of the organogels was measured by dipping the glass electrode of the pH meter into the samples. The pH of topical drug delivery preparations should lie in the range of 4.5–6.0 (skin pH), to avoid irritation to the skin.[35]

Hemocompatibility test

The hemocompatibility test was carried out to find out the extent of hemolysis in the presence of the organogel samples. [36–43] Organogels were equilibrated with 50 mL of normal saline (0.9% w/v; 37°C, 30 min). 0.5 mL of the equilibrated sample was diluted with 0.5 mL of diluted blood (prepared by diluting 8 mL of citrated blood with10 mL of normal saline) and the final volume was made up to 10 mL with normal saline. Similarly, a set of positive control was prepared by mixing 0.5 mL of diluted blood with 0.5 mL of 0.1*N* hydrochloric acid to induce complete hemolysis and subsequently diluted to 10 mL. For negative control, 0.5 mL of blood was diluted to 10 mL with normal saline. The samples were then incubated for 1 h at 37°C and then centrifuged at 3000 rpm for 10 min. Optical density (OD) of supernatant was determined at 545 nm using spectrophotometer (Systronic 2203). The percentage of hemolysis was calculated as per the following formula:

$$\% \text{ Hemolysis} = \frac{\text{OD}_{\text{test}} - \text{OD}_{\text{negative}}}{\text{OD}_{\text{positive}} - \text{OD}_{\text{negative}}} \times 100 \qquad (1)$$

In vitro drug release studies

The *in vitro* drug release study gives a valuable insight about the *in vivo* release behavior. A two-compartment vertical diffusion cell arrangement was used for the drug release study. The receptor had a capacity of 50 mL while the donor had a capacity of 10 mL. The diffusion area was 7 cm^2. A dialysis membrane (MW cut off: 60 kDa, Himedia, Mumbai) was used as the semipermeable membrane and was secured to the donor. Accurately weighed 1 g of SA-loaded organogel was poured in the donor. The donor was subsequently lowered such that the dialysis membrane just touched the receptor fluid (50 mL of double distilled water). The receptor fluid, maintained at 37 ± 0.5°C, was stirred at 100 rpm on a magnetic stirrer-cum-hot plate (Remi India Ltd). At intervals of 15 min for the first hour and 30 min for the subsequent 7 h, the volume of the receptor was completely replaced with fresh volume of water. This helped in maintaining sink conditions during the drug release studies. Aliquots of 5 mL was withdrawn from the replaced fluid and measured spectrophotometrically (Systronic 2203) at λ_{max} 277 nm. All the experiments were carried out in duplicate. Data obtained was analyzed by applying various drug release kinetic models, so as to find out best fit model.

Antimicrobial evaluation

Antimicrobial assay was used to determine the suitability of the gels to be used as vehicle for controlled drug delivery. Two strains of bacteria *E. Coli* and *B. Subtilis* were used to analyze the antimicrobial efficacy of the SA-loaded organogel. Broth cell suspension (1 mL) containing 10^{-6}–10^{-7} cfu/mL was spread on plates with solid nutrient agar using a sterilized spreader. Wells of diameter 5 mm were drilled in the plates using a borer so as to accommodate 0.5 g of organogel loaded with drug. The plates were then incubated at 37°C for 24 h and zone of inhibition was measured using scale after completion of incubation period.

RESULTS AND DISCUSSION

Preparation of organogels samples

Span-60 was dissolved in SO, which was kept at 60°C and stirred at 500 rpm, so as to obtain a clear homogenous solution. As the temperature of solution was lowered, span-60 started precipitating out of the SO due to the change in its solubility parameter. The precipitated span-60 crystals started growing in size as fibers. These fibers physical interacted with each other to form a three-dimensional networked structure.[44] During the process, the clear homogenous solution turned into a cloudy solution, which on further standing either remained as fluid (Fig. 1) or formed yellowish-white or white gels (Fig. 2). The samples were regarded as organogels, if the cloudy solution did not flow when cooled to RT.[28,29] CGC is the minimum concentration of gelator that has the ability to structure the apolar

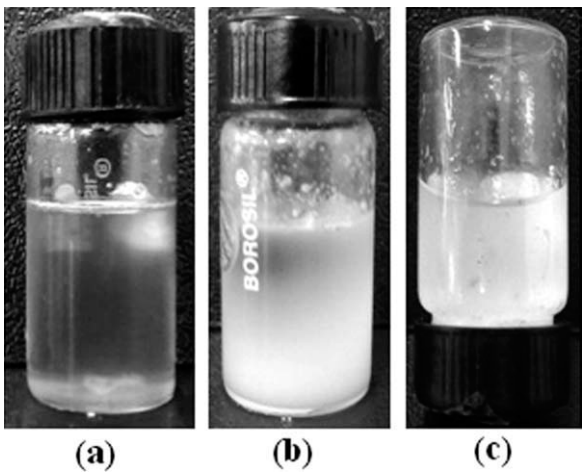

Figure 1 Solution of 15% (w/w) span-60 in SO (a) clear solution after heating at 60°C; (b) turbid suspension upon cooling and standing; (c) Upon further cooling and standing, suspension flowing on inverting the culture bottle.

phase.[45] The results indicated that the CGC of the organogelator was 18 % (w/w). The organogels used for further analysis have been tabulated in Table I.

Organoleptic evaluation

The samples were found to be yellowish-white in color (Fig. 3). Sample A lost its consistency when agitated with hand. As the concentration of the organogelator was increased, the consistency of the products increased. Incorporation of SA slightly improved the consistency of the sample A. All the samples were found to be oily to touch and were having gritty nature. The blank organogels were having a bland taste whereas SA-containing organogels were having slightly acidic taste.

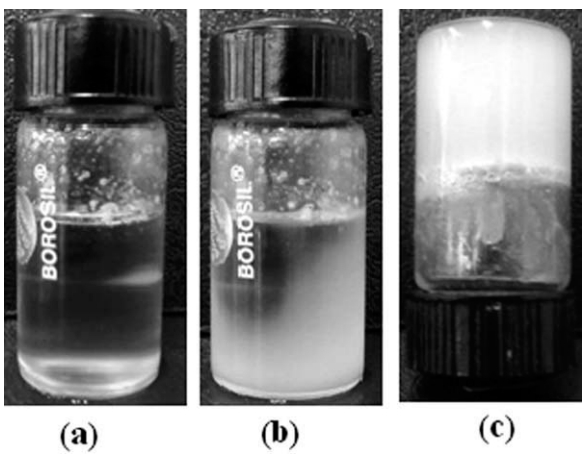

Figure 2 Gelation process of organogel containing 18% (w/w) span-60 in SO; (a) clear solution after heating; (b) uniform, cloudy suspension upon cooling and standing; (c) opaque, semi-solid gel upon further standing.

TABLE I
Composition of the Organogels Used for Analysis

	Concentration of various components (% w/w)	
Sample code	Span-60	SO
A	18	82
E	21	79
F	23	77
H	25	75
AD (1% SA)	18	82
HD (1% SA)	25	75

Accelerated ageing studies

Accelerated ageing test was carried out by thermocycling method. The method involved incubation of the samples alternatively at higher (60°C) and lower (−20°C) temperatures. This study helped in the prediction of mechanism of gel destabilization due to the change in the physiochemical properties at the extreme conditions. At higher temperatures, the chances of oxidative changes are predominant which alter the stability of the samples whereas at lower temperatures, the formation of solidified structures may change the physical interactions amongst the sample components which, in turn, may alter the stability of the samples. This method only gives a prediction about the stability.[46] In general, it is expected that the samples should withstand at least five cycles of freeze–thawing process to be regarded as stable samples.[47] All the samples (mentioned in Table I) were found to be stable for more than 16 cycles without any signs of destabilization.

Stability studies on time scale

The duration of the time period for which a gel maintains its integrity, without any separation of the solid and the liquid phases, when stored in sealed vials at a given environmental condition helps in predicting the shelf-life of the product at the given

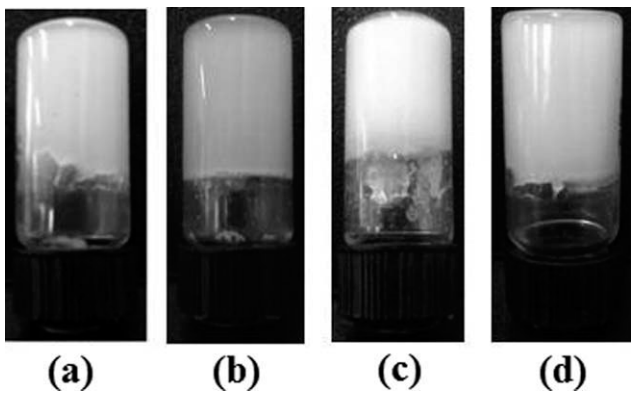

Figure 3 Span-60-based organogels; (a) A, (b) E, (c) F, and (d) H.

TABLE II
Results of Stability Studies on Time Scale

Sample	Destabilization time (months)		
	Ambient temperature	At 5°C	At 40°C
A	12	12	1
E	12	12	1.5
F	12	12	1.5
H	12	12	1.5

condition.[48] To determine the lifetime of the organogels under different environmental conditions, the samples were kept at 5°C, 40°C and at ambient temperatures (25°C). The results (Table II) indicated that when the samples are stored at 40°C, the samples destabilized within a span of 1.5 months whereas the samples kept at 5°C and RT were found to be stable during the experimental period of 12 months. The results suggested that the stability of samples may be prolonged if they are stored at lower temperatures and may be tried as drug-delivery vehicles with sufficient shelf-life.[49]

Gel–sol transition

The gel–sol transition is an important physical phenomenon with considerable scientific and industrial importance.[50] It is, sometimes, also referred to as gel melting temperature (T_gs) and is an important parameter for gel stability and shelf-life.[51] Gel–sol transition corresponds to the deformation and subsequent disruption of the three-dimensional networked structures above a critical temperature. The disruption in the three-dimensional structures result in the increase in the translational mobility of the cross-linked polymer chains.[52] The gel–sol transition was determined by inverting tube method. Visual method of determination of gel–sol transition temperature gave a merely rough idea about T_gs as compared to other methods. It was found to be concentration dependant. As the concentration of span-60 was increased, there was a subsequent rise in the T_gs (Table III). At a higher concentration of the gelator, there was an increase in thermal stability which may be attributed to the increased entanglement of the gelator fibers, responsible for the formation of three-dimensional structure. The rise in temperature increased the surface active energy with a subsequent increase in the mobility of self-assembled aggregates formed by the gelator molecules. This resulted in the interference of absorbed thermal energy with the molecular interactions amongst self-assembled aggregates.[53] This in turn resulted in the disruption of the networked structure thereby causing the system to flow freely (Fig. 4). Gel–sol transition temperature (T_g) of the organogel containing 24 and 25 % (w/w) span-60 was found to be more than that of others. This may be attributed to the requirement of more heat energy required for the disruption of the more densely packed network structure as the gelator proportion was increased.

TABLE III
Results of gel-sol Transition

Sample	T_gs (°C)
A	54
E	56
F	56
H	60

Microscopic studies

Microstructure analysis was carried out to determine the distribution of tubular aggregates with varying proportions of gelator (Fig. 5). The results showed the presence of needle shaped crystals of span-60 in SO when 5 % (w/w) gelator concentration was used (Fig. 5). As the concentration of the gelator was increased, these clusters aggregated to form fiber-like structures. The density of these fiber-like structures increased with the increase in the gelator concentration. As the CGC was reached, these fiber-like structures were found to form networked skeleton which helped in the immobilization of the SO.

Figure 4 Gel–sol transition; (a) Sample A at 30°C and (b) Sample A at 55°C.

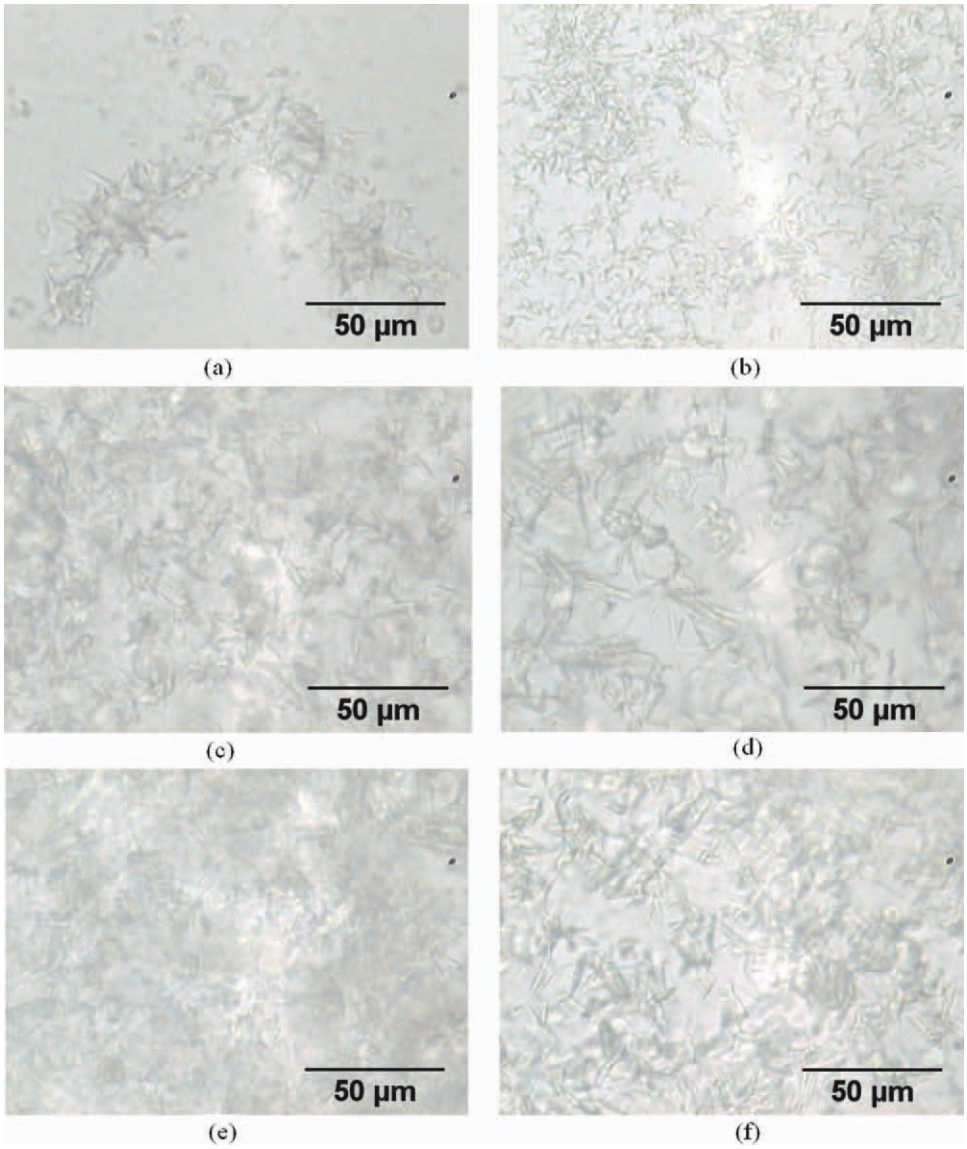

Figure 5 Micrographs of span-60/SO mixtures at RT. (a) 5% (w/w), (b) 10% (w/w), (c) 15% (w/w), (d) 18% (w/w), (e) 20% (w/w), (f) 22% (w/w).

FTIR analysis

Sample A and AD were taken as the representative organogel samples. Figure 6 shows the FTIR spectrogram of span-60, SO, sample A and sample AD, whereas the FTIR spectra of SA[54] has been given elsewhere. FTIR spectroscopy indicated the presence of molecular interactions amongst the components present in the sample. The spectra of the A and AD samples were found to be similar. SO also showed a similar spectra as that of sample A and AD except the absence of the broad peak in the range of 3700 cm^{-1}–3100 cm^{-1}. This suggested the presence of stretched hydrogen bonded O—H groups in the samples A and AD indicating the presence of intermolecular hydrogen bonds, which play an important role in formation of solid fiber organogels.[55] Peaks observed for sample AD were more intense than that of sample A which might be attributed to the presence of SA within its structure. The characteristic functional groups stretches indicate the presence of alkane (3008 cm^{-1}, and 2922 cm^{-1}), *N*-methyl (2853 cm^{-1}), saturated ester (1743 cm^{-1}), and C—O stretch (1160 cm^{-1}) in the raw materials and the samples.[34,56]

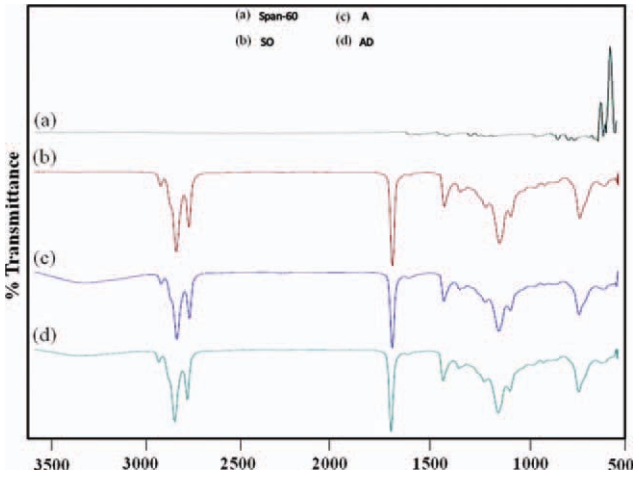

Figure 6 Graph showing results of FTIR analysis; (a) span-60, (b) SO, (c) A, and (d) AD. [Color figure can be viewed in the online issue, which is available at wileyonlinelibrary.com.]

XRD analysis

XRD reveals information about the interactions at the molecular level which changes crystallinity of a given sample.[57–59] Effect of incorporation of SA and thermo-cycling on the crystallinity of the samples was also studied. To study this effect, the representative samples A, H, AD, and HD were chosen since there were not significant changes in the properties amongst the rest of the samples as compared to samples H and HD. The sample H was renamed as HT after the accelerated ageing studies. The XRD profiles have been shown in Figure 7. The full widths at half maximum (FWHM) and area under the curve (AUC) for the analyzed samples have been tabulated in Table IV.

The presence of a single broad peak at 20° 2θ for all the blank organogels and drug loaded organogels indicate amorphous dominant nature of the samples with low crystallinity. Crystallinity of organogels may be attributed to the presence of network structure made up of solid fibers of span-60 formed in SO. SA showed three sharp peaks at 10°, 18°, and 30° 2θ indicating its crystalline nature. But as SA was incorporated in the gels no peaks corresponding to SA was found. This can be explained by the solubility of SA in the oil fraction of gels.[60] SA used in the composition of organogel got uniformly dissolved in the SO which is entrapped within the

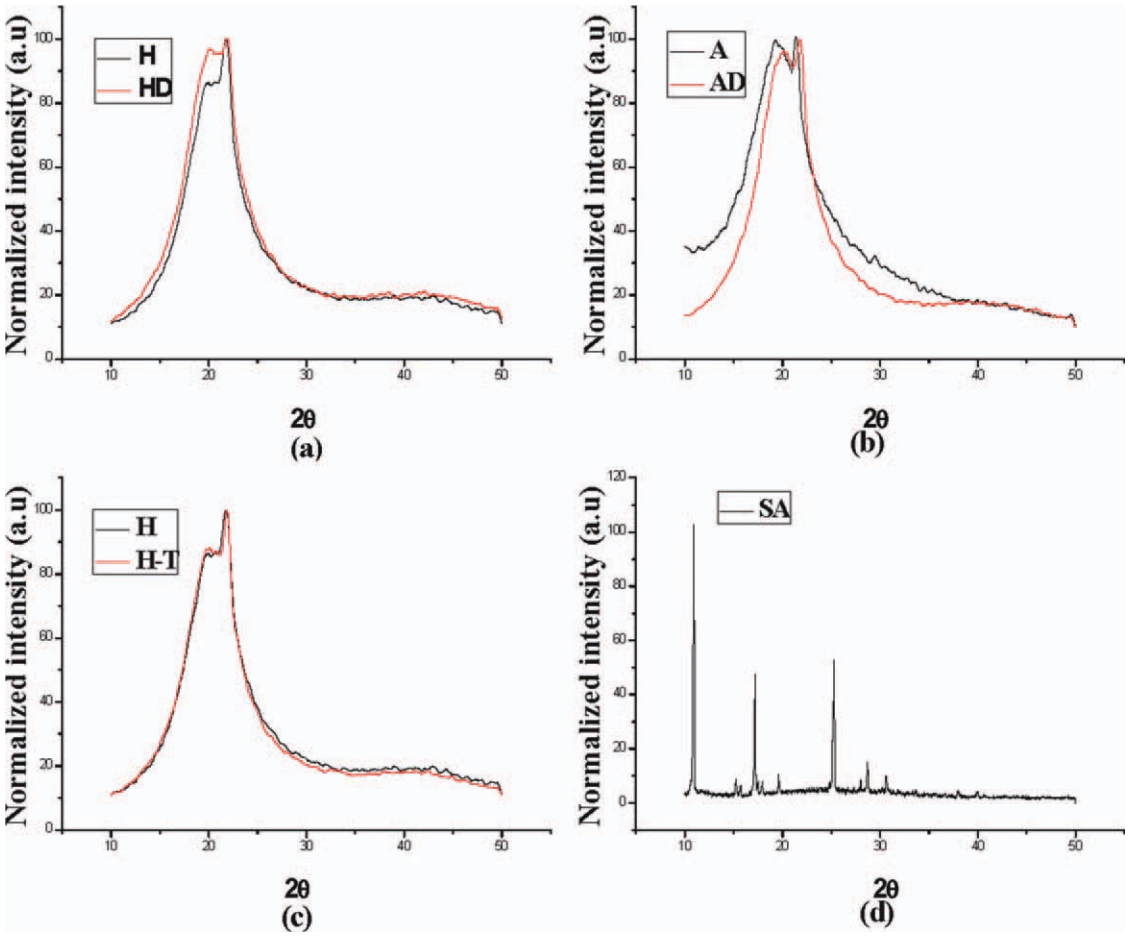

Figure 7 XRD data of the organogel samples; (a) H and HD, (b) A and AD, (c) H and H-T, and (d) SA. [Color figure can be viewed in the online issue, which is available at wileyonlinelibrary.com.]

TABLE IV
Values of AUC and FWHM for XRD Studies

Sample	AUC	FWHM
H	431.53	6.24
HD	556.06	6.92
H-T	473.16	6.24
A	687.45	9.00
AD	532.82	6.72

gelator network. Hence, the crystals of SA are not available responsible for the characteristic peaks. Incorporation of SA slightly decreased the crystalline nature of the sample H evident from the increased FWHM and AUC (Table IV). On the other hand, the crystallinity of the sample A increased with the incorporation of the SA. This explained the improved consistency of the sample A as SA was incorporated. The increase in the crystallinity of the gels may decrease the rate of release of a drug from the delivery matrix.[61] Since the FWHM of the sample AD and HD were almost comparable, it may be estimated that the release of SA from the organogels will not vary significantly. The effect of thermocycling on the crystallinity of the gels was also studied. The XRD profile of the sample H indicated that there was not much change in the crystallinity of the sample H even after accelerated aging stability tests (sample HT).

Opacity measurement

The changes in the absorbance of the organogels as the hot solutions of span-60/SO were cooled at RT have been shown in Figure 8. It was found that at the same temperature, the sample with higher concentration of span-60 showed a higher absorbance than that of the sample with lower concentration of the organogelator. As the concentration of the gelator was increased in the sample, quicker saturation in the OD was observed. This indicated that the rate of precipitation of the span-60 was concentration dependent. As the concentration of gelator increased, the precipitation rate also increased thus supporting the observation of relatively quick gelation of samples with higher concentration of span-60. Sol–gel transition was found out by linear curve fitting of the absorption points in the linear region (Fig. 8). The point of intersection of the linear curves was taken as the sol–gel transition. The sol–gel transition was found to be 54.47°C, 55.09°C, 55.13°C, and 58.59°C for samples A, E, F, and H, respectively.

The change in the absorbance of the gels as a function of time has been shown in Figure 9. Results showed that as the gelator concentration was increased, the absorbance of the solution was higher at a particular instance of time. This suggested that as the solutions were cooled at RT, the rate of precipitation of the gelator was higher in samples with higher proportions of organogelators.

Thermal Analysis

The simultaneous DTA-TGA thermogram profile of the sample A has been shown in Figure 10. DTA thermogram showed a melting endotherm of sample A at 58.34°C. A subsequent exothermic peak corresponding to weight loss, obtained from TGA thermogram, was observed at ~ 196°C. This might

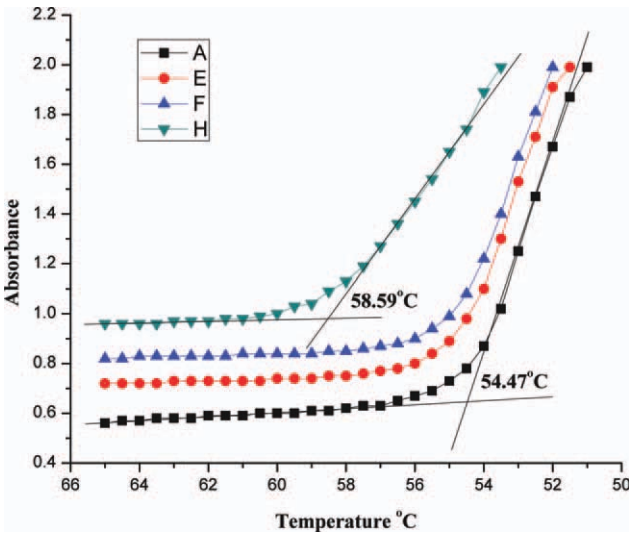

Figure 8 Change in absorbance of hot span-60 in SO solution as the temperature was varied. [Color figure can be viewed in the online issue, which is available at wileyonlinelibrary.com.]

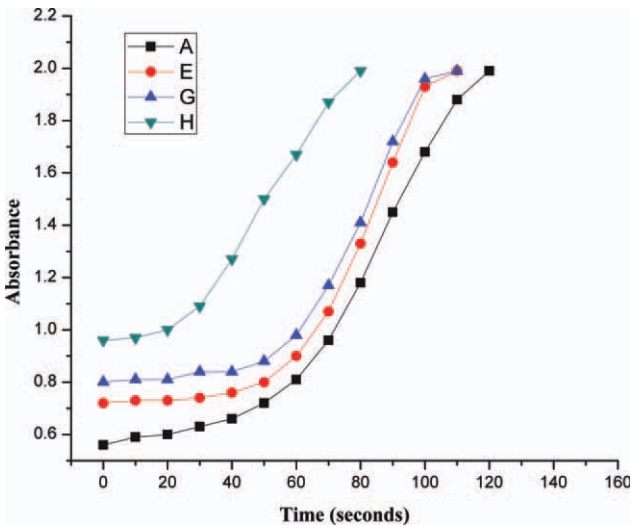

Figure 9 Change in absorbance of hot span-60 in SO solution as a function of time as the samples were kept at RT. [Color figure can be viewed in the online issue, which is available at wileyonlinelibrary.com.]

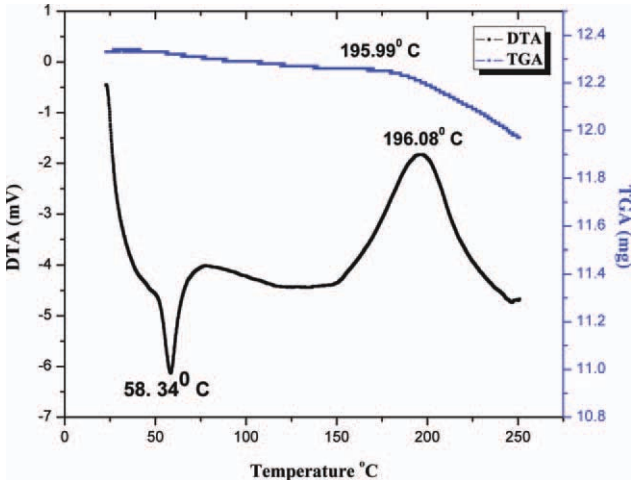

Figure 10 Simultaneous TGA-DTA thermogram of organogel A. [Color figure can be viewed in the online issue, which is available at wileyonlinelibrary.com.]

be attributed to release of heat energy due to the degradation of the sample components.

The samples H, A, HD, and AD were subjected to thermal analysis, using a differential scanning calorimeter, in the temperature range of 29–80°C. Characteristic endothermic peaks were observed in DSC thermograms of H, HD, A, and AD which represent the gel–sol phase transformation. The results indicated that with the increase in the gelator concentration, there was a subsequent increase in the melting endotherm. The melting endotherm of sample AD was found to be higher than the sample A, whereas the melting endotherm of sample HD was found to be lower than sample H, Figure 11. This may be explained by the XRD results, which suggested that the crystallinity of the sample AD was higher than sample A and the crystallinity of sample HD was lower than sample H. In general, higher the crystallinity, higher was the melting temperature.[62]

pH measurement

The pH values of the organogel samples were found to be in the range of 5.5–6.7 (Table V), which is in close to skin pH 4.5–7.[35,63–66] This indicated that the samples may not cause any irritation to the skin and hence can be used for topical applications.

Hemocompatibility test

The percentage hemolysis of goat RBCs was measured in the presence of the sample leachant and has been tabulated in Table VI. The results suggested that all the organogel samples were highly hemocompatible (% hemolysis < 5 %) and may be regarded as biocompatible in nature.[37]

In vitro drug release studies

Figure 12 shows the release profile of SA from the prepared gels. Drug release from a formulation depended upon its solubility and partition coefficient in oil and water.[67] The mechanism and kinetics of drug release were analyzed by different mathematical models, e.g., zero order (1), first order (2), Higuchi (3), Hixon–Crowell, Weibull, Korsemeyer–peppas (4).[68–70]

$$Q = k_0 t \tag{1}$$

$$\ln Q = \ln Q_0 - k_1 t \tag{2}$$

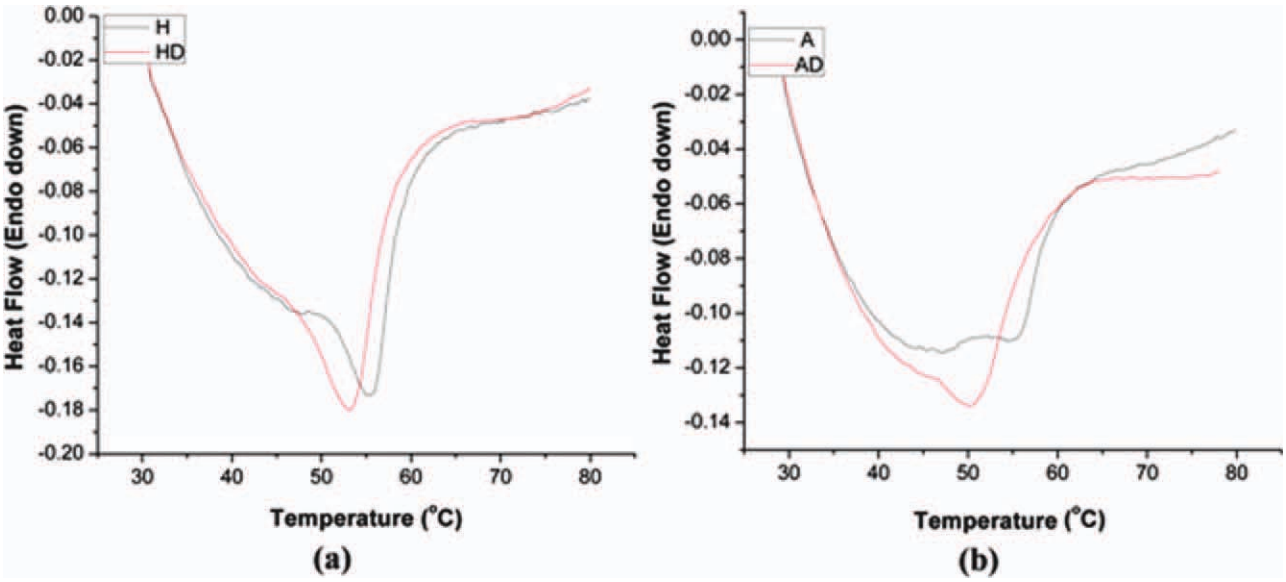

Figure 11 DSC thermogram of organogels; (a) H and HD, (b) A and AD. [Color figure can be viewed in the online issue, which is available at wileyonlinelibrary.com.]

TABLE V
pH Values of Organogel Samples

Sample code	pH
A	5.90 ± 0.30
E	5.50 ± 0.30
F	5.70 ± 0.15
H	6.10 ± 0.30

$$Q = k_H t^{1/2} \quad (3)$$

$$M_1 + M = k_p t^n \quad (4)$$

where Q is the cumulative percent of drug released at time t, M_t/M is the fraction of drug released at time t, and k_0, k_1, k_H, k_p, and k are the rate constants for respective models. Q_0 is a constant and n is the diffusion exponent constant.

The effect of gelator concentration on the release of drug was studied. The results indicated that the drug diffusion can be controlled by varying the concentration of gelator. Samples AD and HD represent samples A and H with drug. The amounts of drug released from the AD, and HD samples were found to be ~ 40% and ~ 36%, respectively, at the end of 8 h. This suggested that as the amount of gelator was increased, there was a subsequent reduction in the drug release rate. This indicated that the drug release was dependent on the solid skeleton network formed by the gelator molecules.[17,71] Recent studies have also reported that self association or assembly of fatty acid surfactants (span 60) limits the diffusion of drug across the gel matrix.[72]

Table VII shows the drug release rate constant (k) and coefficient of determination (r^2) determined for different kinetic models of drug release. The release kinetics best-fit model indicated that the release of the drug from the organogels followed Higuchi Model kinetics (Fig. 13 and Table VII), indicating that the organogels may be used as controlled delivery systems. Korsmeyer–Peppas model was used to figure out the Fickian constant "n." The n value was found to be in between 0.5 and 0.7, suggesting that the release mechanism was a combination of both fickian and non-fickian kinetics.

TABLE VI
Results of the Hemocompatibility Test

Sample	Hemolysis (%)
A	0.85
AD	1.25
H	0.98
HD	1.32

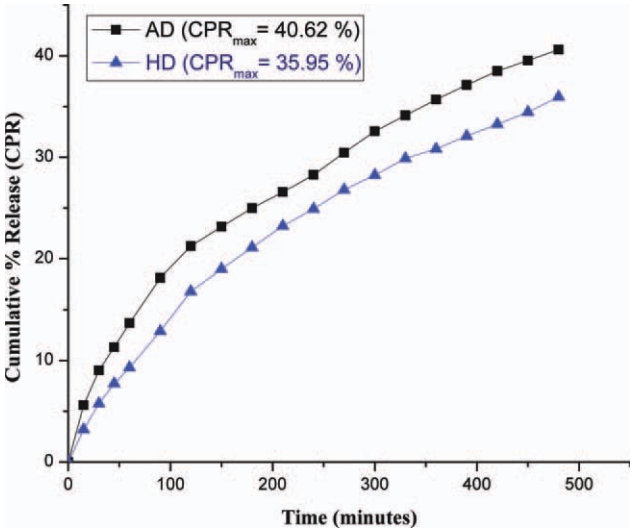

Figure 12 CPR values for different compositions of the organogel samples as a function of time. [Color figure can be viewed in the online issue, which is available at wileyonlinelibrary.com.]

It can be concluded from the above that the A and H samples may be tried as a matrix for controlled release, which have been quite often associated with the solid fiber organogels.[17,71]

Antimicrobial evaluation

The sample A acted as a negative control whereas the sample AD was used as the test sample for the antimicrobial efficacy of the formulation against *E. coli* and *B. subtilis*. The zone of inhibition was measured after 24 h of incubation of the microbes in the presence of the organogels. The antimicrobial activity after the incubation period has been shown in Figure 14 and the results have been tabulated in Table VIII. The sample AD was able to inhibit the growth of both the microorganism even after 24 h in the neighborhood zone (Table VIII). On the other hand, the sample A did not show any zone of inhibition. This suggested that the antimicrobial activity of the sample AD is due to the presence of SA in the formulation.

CONCLUSIONS

A new class of thermoreversible organogels were developed using span-60 and SO. Span-60, a major nonionic surfactant, has been widely used in food and cosmetic industries as an emulsifier may be tried as a matrix for controlled delivery of various pharmaceutical agents. Its unique property to gel edible oil has been utilized in this study to develop transdermal formulation. Microscopic studies indicated that small needle-shaped clusters aggregated

TABLE VII
Kinetics of Drug Release

	r^2, k, and n values for in vitro drug release kinetics											
	Zero order		First order		Higuchi model		Hixon–Crowell model		Weibull model		Korsmeyer peppas model	
Sample	r^2	K_0	r^2	K_1	r^2	k_H	r^2	k_{HC}	r^2	K_W	r^2	n
AD	0.922	0.001	0.0390	$5.422E^{-4}$	**0.998**	1.914	0.019	$8.598E^{-4}$	0.846	1.119	0.995	0.592
HD	0.949	0.001	0.045	$5.898E^{-4}$	**0.993**	1.775	0.025	$9.923E^{-4}$	0.895	1.147	0.988	0.619

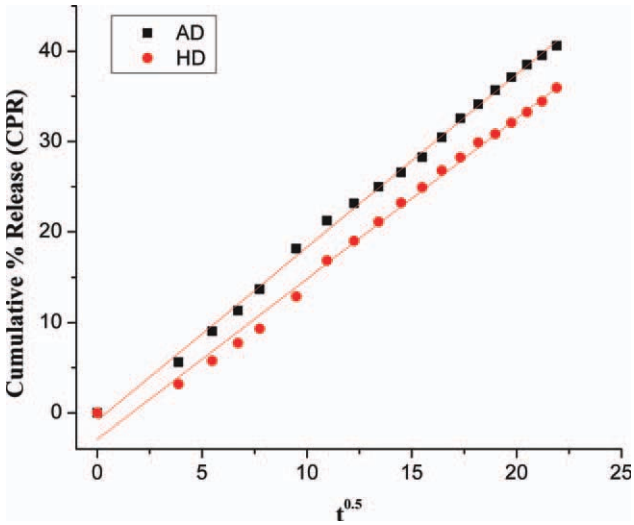

Figure 13 Higuchian-model kinetics for the different organogels samples; (a) AD, and (c) HD. [Color figure can be viewed in the online issue, which is available at wileyonlinelibrary.com.]

to form fibers, which underwent interaction amongst each other to form a networked structure. The networked structure helped in the immobilization of

TABLE VIII
Results of Antimicrobial Screening Test

	Zone of inhibition (diameter; cm)		
Bioactive agent	*E. coli*	*B. subtilis*	Control
Salicylic acid 1 % (w/w)	1.1 ± 0.2	1.1 ± 0.3	nil

the SO. Stability studies showed that the samples were stable at harsh condition that makes it suitable for formulating delivery vehicles with prolonged shelf-life. The drug release could be modulated by altering the proportion of gelator. With the increase in the gelator concentration, there was a subsequent decrease in the rate of release of SA from the gels. This phenomena may be used for devising formulations for drugs with short half-life and undergoing rapid metabolism thereby prolonging the duration of bioavailability at the site of action. The pH of the organogels suggested that the organogels might be nonirritant in nature. The organogels were found to be biocompatible in nature and hence may be tried as a matrix for controlled drug delivery.

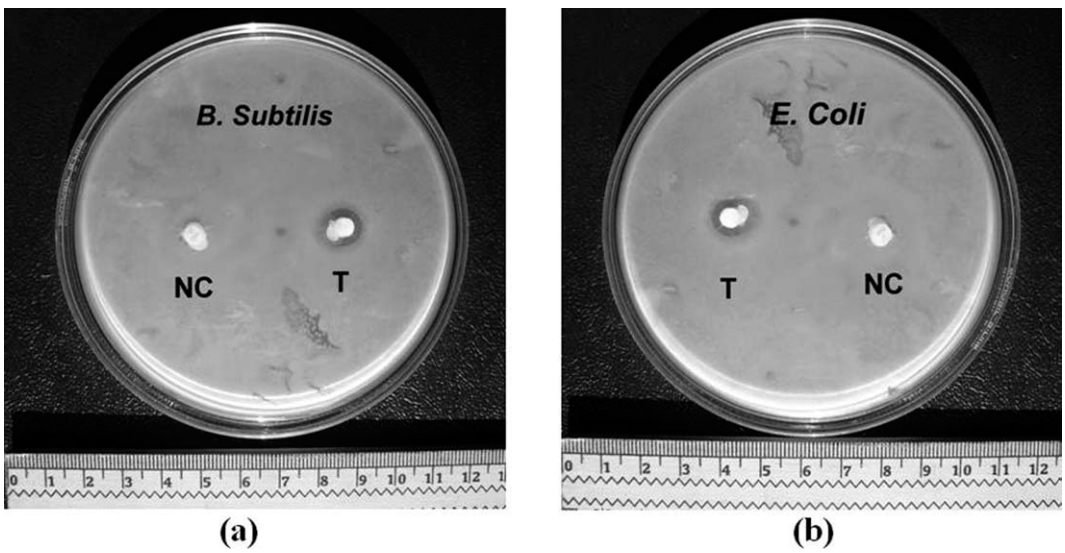

Figure 14 Effect of samples A and AD on the microbial growth (a) *B. subtilis*, and (b) *E. coli*. T = Test (sample AD) and NC = negative control (sample A).

References

1. Kishimura, A.; Yamashita, T.; Aida, T. J Am Chem Soc 2005, 127, 179.
2. scartazzini, R.; Luisi, P. L. J Phys Chem 1988, 92, 829.
3. Bot, A.; Den Adel, R.; Roijers, E. C. J Am Oil Chem Soc 2008, 85, 1127.
4. Duffy, N.; Blonk, H. C. G.; Beindorff, C. M.; Cazade, M.; Bot, A.; Duchateau, G. S. J Am Oil Chem Soc 2009, 86, 733.
5. Toro-Vazquez, J.; Morales-Rueda, J.; Dibildox-Alvarado, E.; Charo-Alonso, M.; Alonzo-Macias, González-Chávez, M. J Am Oil Chem Soc 2007, 84, 989.
6. Hoffman, S.; Yoder, A.; Trepanier, L. J Vet Pharmacol Therap, 2002, 25, 189.
7. Terech, P.; Ostuni, E.; Weiss, R. J Phys Chem 1996, 100, 3759.
8. Richards, H.; Thomas, C. P.; Bowen, J. L.; Heard, C. M. J Pharm Pharmacol 2006, 58, 903.
9. Hughes, N. E.; Marangoni, A. G.; Wright, A. J.; Rogers, M. A.; Rush, J. W. E. Trends Food Sci Technol 2009, 20, 470.
10. Rogers, M. A.; Wright, A. J.; Marangoni, A. G. Soft Mat 2009, 5, 1594.
11. Schaink, H.; Van Malssen, K.; Morgado-Alves, S.; Kalnin, D.; Van der Linden, E. Food Res Int, 2007, 40, 1185.
12. Kantaria, S.; Rees, G. D.; Lawrence, M. J. J Control Release, 1999, 60, 355.
13. Motulsky, A.; Lafleur, M.; Couffin-Hoarau, A. C.; Hoarau, D.; Boury, F.; Benoit, J. P.; Leroux, J. C. Biomaterials 2005, 26, 6242.
14. Murdan, S. Exp Opin Drug Deliv 2005, 2, 489.
15. Terech, P.; Weiss, R. G. Chem Rev 1997, 97, 3133.
16. Sahoo, S.; Kumar, N.; Bhattacharya, C.; Sagiri, S.; Jain, K.; Pal, K.; Ray, S.; Nayak, B. Desig Monom Polym 2010, 14, 95.
17. Vintiloiu, A.; Leroux, J.-C. J Control Release 2008, 125, 179.
18. Murdan, S.; Gregoriadis, G.; Florence, A. T. Eur J Pharm Sci 1999, 8, 177.
19. Nasr, M.; Mansour, S.; Mortada, N. D.; Elshamy, A. J Microencapsulation 2008, 25, 499.
20. Bastiat, G.; Plourde, F.; Motulsky, A.; Furtos, A.; Dumont, Y.; Quirion, R.; Fuhrmann, G.; Leroux, J.-C. Biomaterials 2010, 31, 6031.
21. Pernetti, M.; Van Malssen, K. F.; Flöter, E.; Bot, A. Curr Opin Colloid Interf Sci 2007, 12, 221.
22. Tarrago-Trani, M. T.; Phillips, K. M.; Lemar, L. E.; Holden, J. M. J Am Diet Assoc 2006, 106, 867.
23. Racette, S. B.; Spearie, C. A.; Phillips, K. M.; Lin, X.; Ma, L.; Ostlund, R. E., Jr. J Am Diet Assoc 2009, 109, 2043.
24. Holliday, R.; Phillips, K. Cereal Foods World 2001, 24, 205.
25. Chandrashekar, P.; Lokesh, B. R.; Gopala Krishna, A. G. Food Chem 2010, 123, 728.
26. bayda, B.; uslu, H.; Yavuz, I.; Ceylan, I.; Da suyu, M. Oral Microbiol Immunol 2007, 22, 1.
27. Sakunpak, A.; Panichayupakaranant, P Food Chem 2012, 130, 826.
28. Maity, G. C. J Phys Sci 2007, 11, 156.
29. Shaikh, I. M.; Jadhav, S. L.; Jadhav, K. R.; Kadam, V. J.; Pisal, S. S. Curr Drug Deliv 2009, 6, 1.
30. Hou, Q.; Wang, S.; Zang, L.; Wang, X.; Jiang, S. J Colloid Interf Sci 2009, 338, 463.
31. Khoroushi, M.; Motamedi, S. J Dentis Tehran Univ Med Sci 2007, 4, 21.
32. Sansone, F.; Mencherini, T.; Picerno, P.; d'Amore, M.; Aquino, R. P.; Lauro, M. R. J Food Eng 2011, 105, 468.
33. Anand, A.; Arora, M. Insturmental Methods of Chemical Analysis; Himalaya Publishing House: Mumbai, 2007.
34. Guide for Infrared spectroscopy. Available at: http://www.brukeroptics.com/downloads.html 2011. Accessed on May 4, 2011.
35. Bhatia, V. N.; Barber, R. H. J Am Pharm Assoc 1955, 44, 342.
36. Pal, K.; Banthia, A. K.; Majumdar, D. K. AAPS Pharm Sci Tech 2007, 8, 142.
37. Pal, K.; Banthia, A.; Majumdar, D. J Mater Sci: Mater Med 2007, 18, 1889.
38. Pal, K.; Pal, S. Mater Manufact Processes 2006, 21, 325.
39. Pal, K.; Banthia, A.; Majumdar, D. Biomed Mater 2006, 1, 85.
40. Sutar, P. B.; Mishra, R. K.; Pal, K.; Banthia, A. K. J Mater Sci: Mater Med 2008, 19, 2247.
41. Pal, K.; Bag, S.; Pal, S. J Porous Mater 2008, 15, 53.
42. Pal, K.; Bag, S.; Pal, S. Trends Biomater Artificial Organs 2010, 19, 39.
43. Roy, S.; Pal, K.; Thakur, G.; Prabhakar, B. Mater Manufact Processes 2010, 25, 1477.
44. Dastidar, P.; Trivedi, D. R.; Ballabh, A.; Ganguly, B. Chem Eur J 2004, 10, 5311.
45. Shibayama, M.; Hiroyuki, Y.; Hidenobu, K.; Hiroshi, F.; Shunji, N. Polymer 1988, 29, 2066.
46. Lieberman, H. A.; Rieger, M. M.; Banker, G. S. Pharmaceutical Dosage Forms—Disperse Systems; M. Dekker, 1998.
47. Gooch, J. W. Emulsification and Polymerization of Alkyd Resins; Kluwer Academic/Plenum Publishers, 2002.
48. Murdan, S.; Gregoriadis, G.; Florence, A. T. J Pharm Sci 1999, 88, 608.
49. Sobczuk, A. A.; Tamaru, S.; Shinkai, S. Chem Commun (Camb). 2011, 47, 3093.
50. Nishinari, K.; Zhang, H.; Ikeda, S. Curr Opin Colloid Interf Sci 2000, 5, 195.
51. Liu, J.; Yan, J.; Yuan, X.; Liu, K.; Peng, J.; Fang, Y. J Colloid Interf Sci 2008, 318, 397.
52. Job, N.; panariello, F.; crine, M.; Pirard, J.-P.; Léonard, A. Colloids Surf A: Physicochem Eng Asp 2007, 293, 224.
53. Patra, T.; Pal, A.; Dey, J. J Colloid Interf Sci 2010, 344, 10.
54. Pal, K.; Banthia, A.; Majumdar, D. J Biomater Appl 2006, 21, 75.
55. Wang, X.; Zhou, L.; wang, H.; Luo, Q.; Xu, J.; Liu, J. J Colloid Interf Sci 2011, 353, 412.
56. Coates, J. In Encyclopedia of Analytical Chemistry; Meyers, R. A., Ed.; John Wiley & Sons Ltd: Chichester, 2000; pp 10815–10837.
57. Sionkowska, A.; Wisniewski, M.; Skopinska, J.; Kennedy, C.; Wess, T. Biomaterials 2004, 25, 795.
58. Liu, S. G.; Sui, G.; Cormier, R. A.; Leblanc, R. M.; Gregg, B. A. J Phys Chem B 2002, 106, 1307.
59. Sato, H.; Nakamura, M.; Padermshoke, A.; Yamaguchi, H.; Terauchi, H.; Ekgasit, S. Noda, I.; Ozaki, Y. Macromolecules 2004, 37, 3763.
60. Yu, H.; Xiao, C. Carbohydr Polym 2008, 72, 479.
61. Peppas, N. A.; Scott, J. E. J Controll Release 1992, 18, 95.
62. Markovic, N.; Ginic-Markovic, M.; Dutta, N. K. Polym Int 2003, 52, 1095.
63. Schmid-Wendtner, M. H. pH and Skin Care; ABW Wissenschaftsverlag: Berlin, Germany, 2007.
64. Yosipovitch, G.; Hu, J. HMP Commun 2003, 11, 88.
65. Ayushveda. Available at: http://www.ayushveda.com/beautytips/makeup-tips/skin-ph.htm. 2011, Accessed on 01/04/11.
66. Skinbiology. Available at: http://www.skinbiology.com/skinhealth&aging.html. 2011, Accessed on 01/04/11.
67. Zia, H. A.; Aboofazeli, R.; Nasseri, A.; Needham, T. E. Iran J Pharm Res 2003, 2, 117.
68. P. Costa, Sousa Lobo, J. M. Eur J Pharm Sci 2001, 13, 123.
69. Nanjwade, B. K.; Bechra, H. M.; Nanjwade, V. K.; Derkar, G. K.; Manvi, F. V. J Bioanal Biomed 2011, 3, 032.
70. Shoaib Harris, M.; Jaweria, T.; Merchant Hamid A.; Ismail, Y. R. Pak J Pharm Sci 2006, 19, 119.
71. Yang, Y.; Shaoning, W.; Hui, X.; Chengbo, S.; Xuanbin, L.; Junmin, Z. Asian J Pharm Sci 2008, 3, 175.
72. Dew, N.; Bramer, T.; Edsman, K. J Colloid Interf Sci 2008, 323, 386.